Effect of the magnetic impurity on the charge diffusion in highly dilute Ce doped $LaMnO_3$

Cite as: AIP Advances **10**, 015223 (2020); https://doi.org/10.1063/1.5130429
Submitted: 23 October 2019 . Accepted: 20 December 2019 . Published Online: 14 January 2020

G. A. Cabrera-Pasca, B. Bosch-Santos, A. Burimova, E. L. Correa, and A. W. Carbonari

Effect of the magnetic impurity on the charge diffusion in highly dilute Ce doped $LaMnO_3$

Cite as: AIP Advances 10, 015223 (2020); doi: 10.1063/1.5130429
Presented: 5 November 2019 • Submitted: 23 October 2019 •
Accepted: 20 December 2019 • Published Online: 14 January 2020

G. A. Cabrera-Pasca,[1] B. Bosch-Santos,[2] A. Burimova,[2] E. L. Correa,[2] and A. W. Carbonari[2,a)]

AFFILIATIONS

[1] Faculdade de Ciências Exatas e Tecnologia, Universidade Federal do Pará, 68440-000 Abaetetuba, PA, Brazil
[2] Instituto de Pesquisas Energéticas e Nucleares, IPEN-CNEN/SP, 05508-000 São Paulo, Brazil

Note: This paper was presented at the 64th Annual Conference on Magnetism and Magnetic Materials.
[a)] **Electronic mail:** carbonar@ipen.br

ABSTRACT

$LaMnO_{3+\delta}$ is a complex oxide, which, depending on the oxygen excess concentration, presents different crystalline structure and interesting magnetic and electric properties such as colossal magnetoresistance, polaron dynamics, multiferroic behavior, and charge-orbital ordering. This complexity requires different characterization techniques to draw a picture as complete as possible allowing a good understanding of these phenomena. Here, we have used the perturbed angular correlation (PAC) technique to measure hyperfine interactions at La and Mn sites of $LaMnO_{3+\delta}$(δ ~0.15) using ^{140}Ce and ^{111}Cd at La sites as probe nuclei in order to investigate within an atomic scale the magnetic and electric interactions in this compound. The results show that ^{111}Cd nuclei occupy highly symmetric local sites in agreement with a rhombohedral structure. The magnetic hyperfine field (B_{hf}) measured with ^{111}Cd at La sites is very small (B_{hf} = 0.40 T) due to the supertransferred magnetic field from Mn neighbors through oxygen orbitals. On the other hand, ^{140}Ce nuclei at La sites present a saturation field of around 3.7 T much higher than that expected for La sites (due to the weak transfer field by superexchange mechanism). In addition, for temperature range above the magnetic ordering (200-300 K) a dynamic hyperfine interaction was observed characterized by the attenuation parameter $\lambda(T)$ whose temperature dependence allowed to determine the activation energy (E_a) associated to charge transfer. The polarization of the 4*f*-electron of Ce impurities affects the local magnetic field at impurity sites as well as the E_a.

I. INTRODUCTION

$LaMnO_{3+\delta}$ exhibits a complex magnetic behavior such as the colossal magnetoresistance and different magnetic ordering depending on the oxygen concentration given by δ parameter.[1] The stoichiometric compound $LaMnO_3$ with only Mn^{+3} ion is a semiconductor at room temperature that, at the Néel temperature of T_N = 140 K, orders antiferromagnetically[2] also presenting a cooperative Jahn-Teller distortion of MnO_6 octahedra, whereas the replacement of La with alkaline-earth atoms such as Ca, as well as an excess of oxygen in the sample ($LaMnO_{3+\delta}$ with $\delta > 0$), induces the coexistence of Mn^{+3} and Mn^{+4} which reduces the Jahn-Teller distortion increasing symmetry and favoring the ferromagnetic ordering.

$LaMnO_{3+\delta}$ has been investigated by measuring hyperfine interactions with different results and the characterization of the magnetic hyperfine field (MHF) at La and Mn sites is not well established yet for the full range of possible δ values.[3–7] Besides MHF, studies of hyperfine interactions in $LaMnO_{3+\delta}$ have been carried out also by measuring the electric field gradient (EFG) using the time differential perturbed angular correlation (TDPAC) spectroscopy.[6,8] Because it is a nuclear method, TDPAC has a high sensitivity to the magnetic exchange interactions, local crystallographic variations, and charge distributions around the lattice site where probe nuclei are located and consequently can be used to detect the local magnetism, local symmetry changes as well as dynamic processes due to charge movement or spin fluctuations.[9]

In this work we present a first TDPAC study of non-stoichiometric lanthanum manganite $LaMnO_{3.15}$ in the rhombohedral phase with ^{111}In(^{111}Cd) covering the ranges of low and high temperatures in order to get insight on the effects induced by local structure deformations. The results are compared with previous findings[6,8] where Cd probe originated from ^{111m}Cd,

aiming to understand the correlation between the properties of introduced impurity and the behavior of impurity-compound complex. Another probe used in this work to study $LaMnO_{3.15}$ was $^{140}La(^{140}Ce)$ whose advantage is an almost absolute dominance of magnetic interaction allowing an insight on exchange and dynamic phenomena in $LaMnO_{3+\delta}$.

II. EXPERIMENTAL PROCEDURE

The well-known sol-gel Pechini method based on metal citrate polymerization with ethylene glycol with the thermal decomposition of polymeric mixed-metal precursor gel was used to prepare polycrystalline samples of $LaMnO_3$. High-purity metals, La (99.9%) and Mn (99.98%) in stoichiometric quantities were dissolved separately in concentrated HNO_3 to obtain the nitrate solutions. To reduce the higher valence of manganese ions, a few crystals of hydroxylamine hydrochloride were added to the $Mn(NO_3)_3$ solution. The two solutions were mixed together with few drops of ammonium hydroxide added for neutralization. For chelation citric acid was added in molar ratio of 2:1 to metal. Subsequently, ethylene glycol was added to this solution to promote the formation of an organic ester. The final mixture was then stirred magnetically at 373 K to provoke polymerization. Thus obtained homogeneous gel was heated slowly to 820 K and calcined for 30 h in air. The resulting powder was pressed into pellet, sealed in an evacuated quartz tube and sintered at 1100 K for 40 h.

After cooling to RT the pellet was divided into three parts. The first part was characterized by X-ray diffraction, the second was used for PAC measurements with $^{111}In(^{111}Cd)$ probe nuclei introduced into samples by thermal diffusion. A small volume containing approximately 20μCi of carrier-free ^{111}In in the form of indium chloride solution was deposited on the surface of the sample. After drying, the sample was sealed in an evacuated quartz tube and sintered at 1123 K for 16 h. The third part of the pellet was subjected to neutron irradiation in IEA-R1 research reactor (IPEN-CNEN) to produce ^{140}La activity by $^{139}La(n, \gamma)^{140}La$ reaction, since ^{139}La isotope is naturally present in the sample. TDPAC measurements were carried out in the temperature ranges from 15 K to 300 K and from 13 K to 1100 K, respectively, for $^{140}La(^{140}Ce)$ and $^{111}In(^{111}Cd)$ probe nuclei.

A. A brief description of TDPAC

The technique is based on the hyperfine interaction of the nuclear moments of the probe and the extra nuclear magnetic field and/or electric field gradient (EFG). PAC measurements yield the spin-rotation spectra $R(t)$ which is fitted by $-A_{22}\sum_i f_i G^i_{22}(t)$, a model that takes into account the fractional site population of probe nuclei f_i and its respective approximate perturbation function $G^i_{22}(t)$. A_{22} is the angular correlation coefficient, which, for $^{111}In(^{111}Cd)$ and $^{140}La(^{140}Ce)$ equals -0.18 and -0.09, respectively.[10] For magnetic hyperfine interactions, $G_{22}(t) = 0.2 + 0.4\sum_{n=1,2}\cos(n\omega_L t)$. Fitting $G_{22}(t)$ experimental data one can extract $\omega_L = \mu_N g B_{hf}/\hbar$, where μ_N is the nuclear magnetron and g is the nuclear g-factor. Thus the magnetic hyperfine field, B_{hf}, may be estimated. The perturbation function for electric quadrupole interactions is given by $G_{22}(t) = S_{20} + \sum_{n=1,2,3} S_{2n}\cos(\omega_n t)$. The transition frequencies ω_n, as well as S_{2n} coefficients, are the functions of the components of diagonalized EFG tensor, V_{kk}. Assuming $|V_{xx}| \leqslant |V_{yy}| \leqslant |V_{zz}|$, $\omega_n = eQg_n(\eta)V_{zz}/h$, where eQ is the electric quadrupole moment of the probe nuclei and $\eta = (V_{xx} - V_{yy})/V_{zz}$ is the asymmetry parameter. The broadness of frequency distribution is parametrized with $\delta\omega$. For both quadrupole electric and dipole magnetic static interaction models a Lorentz broadening is assumed.

Spectra taken with ^{111}Cd recorded at temperatures above 200 K were fitted with a model considering two types of pure electric quadrupole interaction characterized by different hyperfine parameters. These parameters correspond to two types of distinct local environments. At low temperatures (T ≤ 200 K) spectra were fitted with combined electric quadrupole plus magnetic dipole interactions.

Since for ^{140}Ce probe Q is small, one expects an almost pure magnetic interaction at La site. Therefore, at temperatures below 200 K, the spectra measured with ^{140}Ce were fitted with a model considering pure magnetic dipole interactions with probe nuclei occupying two types of sites with different spin densities. The only exception is the spectrum taken at 13 K which was fitted with a single magnetic dipole interaction.

Further details on TDPAC technique and the experimental procedure may be found elsewhere.[9,11,12]

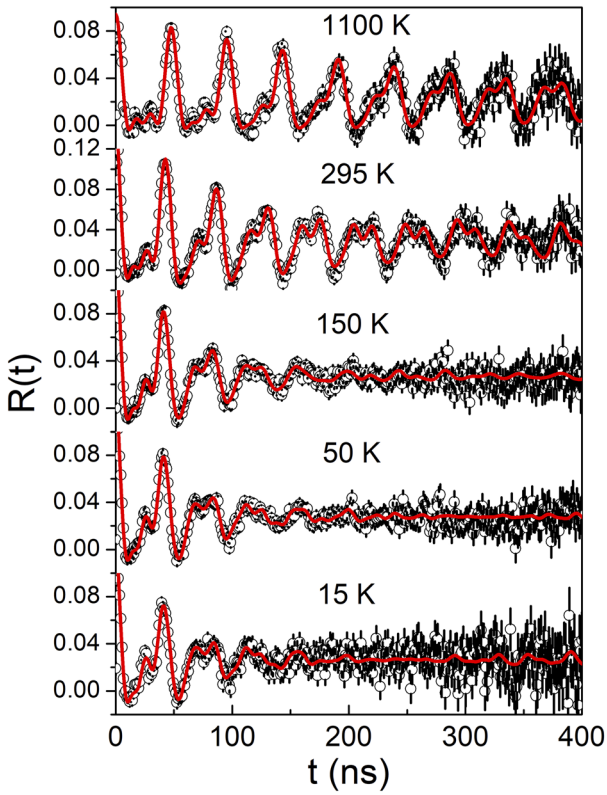

FIG. 1. Spin rotation spectra of $LaMnO_{3.15}$ with ^{111}Cd probe nuclei taken at indicated temperatures. It is possible to observe a slight change in the spectra from 1100 K to 295 K and a stronger change in spectra at low temperatures due to the increase in V_{zz} and η, and the appearance of B_{hf} (below 150 K) as temperature decreases. Solid lines are the least squares fit of the theoretical functions to the experimental data.

III. RESULTS AND DISCUSSION

The X-ray diffraction pattern of polycrystalline $LaMnO_{3+\delta}$ sample taken at RT was analyzed using the Rietveld refinement method. The analysis evidenced the formation the pseudo-cubic crystal structure with space group $R\bar{3}c$ and lattice parameters $a = 5.4663(2)$Å, $\alpha = 60.516(2)^\circ$. Impurity phases Mn_3O_4 and La_2O_3 were observed in minor concentrations. According to Bogush *et al.*[13] and Töpfer *et al.*[1] these values of a and α imply $0.12 < \delta < 0.16$. This range could be narrowed to $0.14 < \delta < 0.16$ considering structural parameters, and local environments of La and Mn in comparison with those found by Tagushi *et al.*[14] Therefore, we consider the oxygen concentration in the samples to be ~0.15.

The spin rotation spectra $R(t)$ taken at different temperatures with ^{111}Cd and ^{140}Ce probe nuclei are displayed in Fig. 1 and 2 respectively. Evident is the change in spectra patterns at low temperatures.

A. TDPAC results for ^{111}In(^{111}Cd) probe nuclei

The results for the temperature dependence of the hyperfine parameters obtained from the fit to the experimental TDPAC spectra measured with ^{111}In(^{111}Cd) are shown in Fig. 3. Calculated values of B_{hf} corresponding to the major fraction are shown in Fig. 4.

At RT, for the major fraction (f = 75%) of probes, $V_{zz}^{(1)} = 81.3(1)$ V/Å^2, $\eta^{(1)} = 0.20$ with narrow frequency distribution ($\delta\omega$ ~3.7%), whereas for the minor fraction $V_{zz}^{(2)} = 86.3(1)$ V/Å^2, $\eta^{(2)} = 0.27$, and $\delta\omega$ ~0.1%. These results for quadrupole intractions are quite different from those reported for $LaMnO_{3.12}$ with ^{111m}Cd as probe nuclei.[6,8] The major fraction of cited previous works, which is assigned to an undistorted environment, presents a higher $V_{zz}^{(1)}$ and a somewhat smaller $\eta^{(1)}$, whereas for the minor fraction, ascribed to a distorted environment, $V_{zz}^{(2)}$ is smaller with a much higher $\eta^{(2)}$. Such highly distorted environment was ascribed to the orthorhombic structure, and wasn't observed in our TDPAC measurements. However, at high temperature, T ~ 800 K, $V_{zz}^{(1)}$ and $\eta^{(1)}$ are, respectively, around 80 V/Å^2 and 0.2 for ^{111m}Cd at the rhombohedral phase in $LaMnO_{3.12}$, as previously reported[8] and are almost similar to our results measured at 800 K as can be seen in Fig. 3. Both results indicate that the local structure for ^{111}Cd in the rhombohedral phase is temperature dependent, rather stronger for higher δ with a noticeable relaxation at high temperatures (present work).

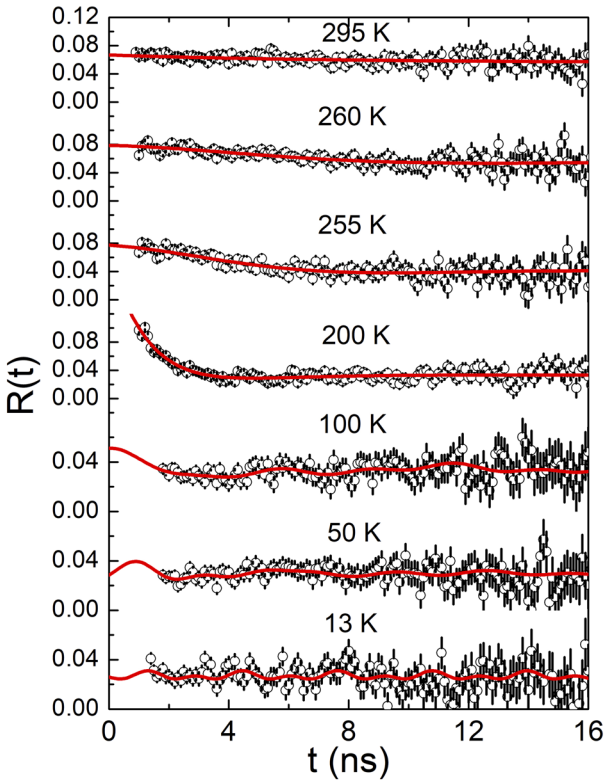

FIG. 2. Spin rotation spectra of $LaMnO_{3.15}$ with ^{140}Ce probe nuclei taken at indicated temperatures. It is clearly seen that the spectra from 200 K to 295 K present a very different behavior from those at low temperatures due to the dynamic interaction and the magnetic dipole interaction, respectively. Solid lines are the least squares fit of the theoretical functions to the experimental data.

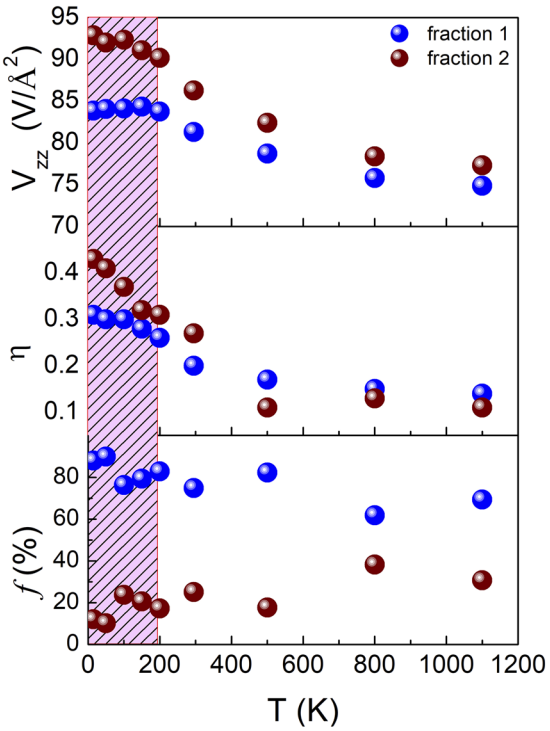

FIG. 3. Temperature dependence of the main EFG component (V_{zz}), asymmetry parameter (η) and site fraction (f) measured in $LaMnO_{3.15}$ with ^{111}Cd for probe nuclei at site fraction 1 (blue spheres) and site fraction 2 (red spheres). Below 200 K (dashed region), due to the presence of combined electric quadrupole plus magnetic dipole interactions, V_{zz} is almost constant for both fractions. Above 200 K, V_{zz} and η decrease and reach a minimum at 600 K indicating a slight change in the local structure.

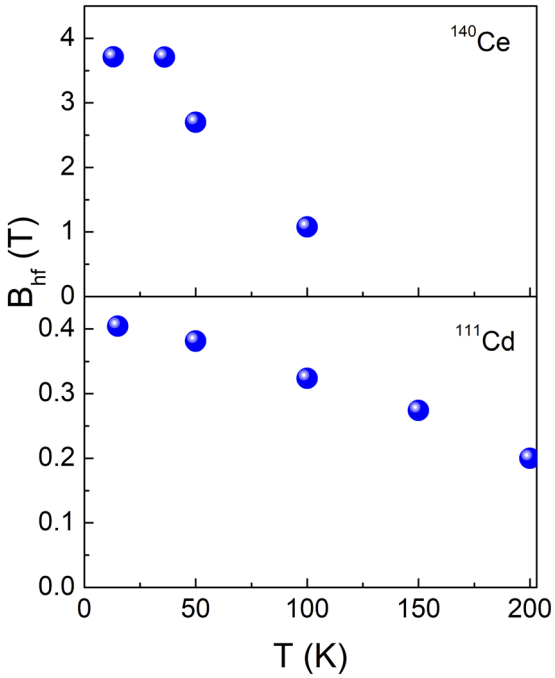

FIG. 4. Temperature dependence of the magnetic hyperfine field (B_{hf}) measured with ^{140}Ce (top) and ^{111}Cd (bottom) in $LaMnO_{3.15}$. The plot at the top indicates that the polarization of Ce impurities has a strong influence on the unusual behavior of B_{hf} vs. temperature.

The observed differences between the measurements with ^{111m}Cd reported by Lopes *et al.*[6,8] and our results with ^{111}Cd are hypothesized to be due to the higher concentration of Mn^{4+} ($\delta > 0.12$) in our samples. Another contribution to this discrepancy may originate from the difference between the valence and ionic radii of probe parents. Compared with La^{3+} (116 pm at higher coordination number), the ionic radius of In^{3+} is ~ 20% smaller, whereas for Cd^{2+} this difference reaches only 5%. If structure relaxation around the probe throughout the decay is relatively slow, local environments of Cd^{2+} originating from ^{111m}Cd and ^{111}In would be different. This assumption remains in accordance with the similarity of the results at elevated temperatures that are expected to catalyze structure rearrangement.

B. TDPAC results for ^{140}La(^{140}Ce) probe nuclei

The temperature dependence of B_{hf} determined from the Larmor frequency of the major fraction obtained from the fit to TDPAC spectra measured with ^{140}Ce, including that at 13 K, is displayed in Fig. 4.

The behavior of B_{hf} for ^{140}Ce with temperature does not follow the expected function similar to the magnetization due to Mn atoms.[1,15] Such an anomalous hyperfine field at ^{140}Ce probe nuclei has been observed for magnetic intermetallic compounds containing rare earth elements where the magnetism comes from Mn atoms[16–19] as well as in magnetic binary and ternary compounds where the magnetic ion is the rare-earth element.[19,20] These anomalies have been attributed to the Ce 4*f* -electron contribution to B_{hf}. In $LaMnO_3$ the anomaly of the temperature dependence of hyperfine field can be attributed to an interaction where *f*-electron of the probe Ce atom is spin polarized by the magnetic field from Mn sublattice and contributes to the effective hyperfine field resulting in an increase of B_{hf} below ~100 K. The value of B_{hf} measured with ^{111}Cd at lowest temperature is very small, around 0.4 T indicating that the spin density transfer from Mn to Cd at La sites through the superexchange interactions is very small, probably due to the unfavored angle in the Mn-O-Cd@La bonds. Therefore, the contribution of *f*-electron of Ce is majoritarian for B_{hf} measured with ^{140}Ce.

Time-dependent interactions are expected due to charge fluctuations[3] and, correspondingly, the TDPAC spectra are characterized by an exponential decay as observed in spectra taken at higher temperatures as can be seen in Fig. 2. In the case of isotropic fluctuations, if the correlation time, *i.e.* the time between two successive dynamic interactions, is much smaller than the spin precession time of the probe nuclei, then $R(t) = e^{-\lambda_k t}$, where λ_k is the relaxation rate of fluctuations. Spectra for $T \leq 200$ K were fitted with this dynamic interaction model. The dynamic interaction observed in TDPAC spectra for ^{111m}Cd was ascribed to the slow diffusion of polarons due to charge motion.[8] The variation of the relaxation rate with temperature is given by $\lambda_k = \lambda_0 \exp[E_a/k_B T]$, where the activation energy, E_a, can be obtained from the linear fit of $\ln \lambda_k(1/T)$, as shown in Fig. 5.

The calculated activation energy is around 0.2 eV which is smaller than E_a ~0.31 eV measured in $LaMnO_{3.12}$ with ^{111m}Cd also at La sites.[8] The reduction in E_a indicates a faster movement of charges. The presence of Jahn-Teller deformation (JTD) in $LaMnO_{3+\delta}$ with $\delta < \sim 0.11$ in the orthorhombic phase stabilizes the antiferromagnetic ordering. With the increase of δ the JTD weakens until for $\delta > 0.12$, it disappears in the rhombohedral phase with a ferromagnetic ordering.[1,21] For $\delta > 0.13$, the polaron regime gives place to fast

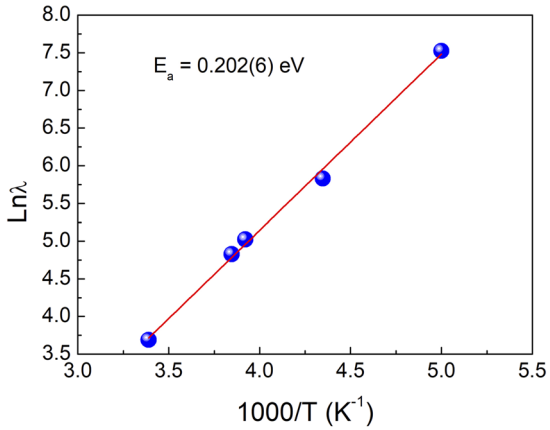

FIG. 5. The logarithm of relaxation rate obtained from the fit of R(t) spectra for ^{140}Ce as a function of the inverse of temperature. The red straight line is the linear fit to the experimental data, from which the activation energy E_a is determined. The large values of λ correspond to fast relaxation.

transfer of charges between Mn^{3+} and Mn^{4+} ions probably through ferromagnetic double exchange interactions.[1] Our data, therefore, shows that ^{140}Ce probes are able to observe faster charge movement than ^{111m}Cd reported by Lopes *et al.*[8] or ^{111}Cd (this work). This is because of the time window for the measurement of the hyperfine interactions of each probe nucleus which is proportional to the half-life of the intermediate level of the excited state used for measurements, 3.4 ns for ^{140}Ce much smaller than 84.5 ns for ^{111m}Cd or ^{111}Cd. The large values of λ observed in the dynamic hyperfine interactions correspond to fast charge transfer between Mn^{3+} and Mn^{4+}, indicanting a metallic behavior. The smaller value of E_a measured with ^{140}Ce when compared to those for slow polaron diffusion[8,22] is ascribed to the influence of the magnetic Ce atom on the charge movement.

IV. SUMMARY

The evolution of spin and charge density distributions in $LaMnO_{3+\delta}$ with δ estimated to be around 0.15 were probed with ^{111}In(^{111}Cd) and ^{140}La(^{140}Ce) at La sites in a wide range of temperatures. TDPAC spectra supported by XRD analysis indicated the presence of a single rombohedral structure for the aforementioned stoichiometry.

Generally, observed characteristics of local environment of Cd@La agree well with the existing results. A slight discrepancy between the electric hyperfine parameters obtained with ^{111}In and those previously reported for ^{111m}Cd probe parent was attributed to charge density deviations induced by the higher number of cation vacancies in our samples.

Results of the magnetic hyperfine field measured with ^{111}Cd, entirely due to the Mn ions, since Cd is a *d* closed-shell atom, show a very weak field, consistent with the ferromagnetic ordering and short Mn-O-Cd(@La) angle unfavoring the superexchange interaction. Results from ^{140}Ce at La sites show that the main contribution, therefore, comes from the Ce 4*f* electron polarized by the neighboring Mn spins. Interestingly, a fast dynamic interaction could be observed by ^{140}Ce in a range of temperatures from 200 K to 295 K and the activation energy for this charge movement could be determined indicating a possible transition between the polaron regime and the fast regime.

Therefore, TDPAC results show that for $LaMnO_{3.15}$ in the rhombohedral phase local structure around ^{111}Cd probe nuclei at La sites experience relaxation from a slight distorted to a more symmetric environment with a very small B_{hf} below 200 K. Additionally, hyperfine interactions at ^{140}Ce probes also at La sites are strongly influenced by the 4*f* electron polarization of Ce impurities that affects B_{hf} as well as the activation energy E_a.

ACKNOWLEDGMENTS

Partial financial support for this work was provided by Fundação de Amparo a Pesquisa do Estado de São Paulo (FAPESP) under grant 2014/14001-1. AWC kindly acknowledges Conselho Nacional de Desenvolvimento Científico e Tecnológico (CNPq) by support in a form of grant 304627/2017-8. AB greatly acknowledges the financial support of FAPESP (grant number 2019/15620-0).

REFERENCES

[1] J. Topfer and J. B. Goodenough, J. Chem. Phys. **130**, 117 (1997).
[2] J. M. D. Coey, M. Viret, and S. von Molnár, Adv. Phys. **48**, 167 (1999).
[3] G. Allodi, M. C. Guidi, R. D. Renzi, A. Caneiro, and L. Pinsard, Phys. Rev. Lett. **87**, 127206 (2001).
[4] P. Ravindran, A. Kjekshus, H. Fjellva, A. Delin, and O. Eriksson, Phys. Rev. B **65**, 064445 (2002).
[5] A. C. junqueira, A. W. Carbonari, R. N. Saxena, and J. Mestnik-Filho, J. Magn. Magn. Mater. **272-276**, e1639 (2004).
[6] A. M. L. Lopes, V. S. Amaral, J. G. Correia, and J. P. Araújo, J. Phys. Condens. Matter **25**, 385602 (2013).
[7] A. Trokiner, S. Verkhovskii, A. Gerashenko, Z. Volkova, O. Anikeenok, K. Mikhalev, M. Eremin, and L. Pinsard-Gaudart, Phys. Rev. B **87**, 125142 (2013).
[8] A. M. L. Lopes, J. P. Araújo, J. J. Ramasco, V. S. Amaral, R. Suryanarayanan, and J. G. Correia, Phys. Rev. B **73**, 100408 (2006).
[9] M. Zacate and H. Jaeger, Defect and Diffusion Forum **311**, 3 (2011).
[10] H. H. Rinneberg, At. Energy Rev. **17:2**, 477 (1979).
[11] A. W. Carbonari, J. Mestnik-Filho, and R. N. Saxena, Defect and Diffusion Forum **311**, 39 (2011).
[12] G. Schatz and A. Weidinger, *Nuclear Condensed Matter Physics: Nuclear Methods and Applications* (Wiley, 1996).
[13] A. K. Bogush, V. I. Pavlov, and L. V. Balyko, Crystal Res. Technol. **18**, 589 (1983).
[14] H. Taguchi, S. Matsu-ura, M. Nagao, and H. Kido, Physica B **270**(3-4), 325 (1999).
[15] M. K. Gubkin, T. A. Khimich, E. V. Kleparskaya, T. M. Prekalina, and A. V. Zalessky, J. Magn. Magn. Mater. **154**, 351–354 (1996).
[16] A. W. Carbonari, J. Mestnik-Filho, R. N. Saxena, and M. V. Lalić, Phys. Rev. B **69**, 144425 (2004).
[17] B. Bosch-Santos, A. W. Carbonari, G. A. Cabrera-Pasca, M. S. Costa, and R. N. Saxena, J. Appl. Phys. **113**, 17E124 (2013).
[18] B. Bosch-Santos, A. W. Carbonari, G. A. Cabrera-Pasca, R. S. Freitas, and R. N. Saxena, J. Appl. Phys. **117**, 17E304 (2015).
[19] G. A. Cabrera-Pasca, A. W. Carbonari, R. N. Saxena, B. Bosch-Santos, J. A. H. Coaquira, and J. A. Filho, J. Alloys and Compounds **515**, 44–48 (2012).
[20] F. H. M. Cavalcante, L. F. D. Pereira, A. W. Carbonari, J. Mestnik-Filho, and R. N. Saxena, J. Alloys and Compounds **660**, 148–158 (2016).
[21] F. Prado, R. D. Sánchez, A. Caneiro, M. T. Causa, and M. Tovar, J. Solid State Chem. **146**, 418–427 (1999).
[22] J.-S. Zhou and J. B. Goodenough, Phys. Rev. B **68**, 144406 (2003).